Measurement of Velocity and Concentration Profiles of Pneumatically Conveyed Particles in a Square-Shaped Pipe Using Electrostatic Sensor Arrays

Xiangchen Qian[1,*], Yong Yan[2], Shitong Wu[1], Shuai Zhang[1,**]

1. School of Control and Computer Engineering, North China Electric Power University, Beijing 102206, China
2. School of Engineering and Digital Arts, University of Kent, Canterbury, Kent CT2 7NT, UK

(* Corresponding author: xqian@ncepu.edu.cn)
(** Dr. Zhang is currently working with State Grid Information & Telecommunication Group Co., LTD., Beijing 102211, China)

Abstract

Cross-sectional measurement of particle velocity and concentration in a pneumatic conveying pipe is desirable for the characterisation of particle flow dynamics and determination of particle mass flow rate. In this study, an inner-inserted electrostatic sensor array consisting of nine pairs of electrodes is implemented to measure the cross-sectional velocity and concentration profiling of particles over the whole cross section in a square-shaped pipe. Experimental tests were conducted on both vertical and horizontal pipe sections on a test rig under dilute conditions with different air velocities and particle mass flow rates. Test results show that the slope-shaped particle concentration profile changes to an arch-shaped one when the particles flow from a horizontal pipe to a vertical one. The particle velocity profile is arch-shaped in both vertical and horizontal pipes. A comparative study of cross-sectional mean particle velocity and concentration measured by the developed electrostatic sensor arrays is conducted.

Keyword: *Flow profile; dilute gas–solid two-phase flow; electrostatic sensor array; square-shaped pipe; pneumatic conveying; flow measurement*

1. Introduction

On-line flow measurement of pneumatically conveyed particles in a square-shaped pipe is indispensable for the optimal control of industrial processes, enhancing productivity and reducing energy consumption [1]. The flow profile of solid particles in a dilute gas–solid transport pipe can be highly inhomogeneous depending upon the pipe orientation, measurement position, phase loading ratio, conveying air velocity and properties of the particles. In consequence, incorrect quantification of the volumetric concentration, velocity and mass flow rate of conveyed particles may be obtained using most of the available measurement and numerical methods [1]. Therefore, measurement of the cross-sectional distribution of particle concentration and velocity is desirable for the characterisation of the dynamics of pneumatically conveyed particles.

Due to the advantages of simple manufacturing and easy installation, square-shaped pipes are commonly used for conveying particles in industrial processes, such as circulating fluidised beds [2], and thermal power plants in Germany, China and some eastern European countries [3], flue gas transportation systems and for ventilation in buildings. However, research on the modelling and measurement of dilute phase particle flow profile within square-shaped pneumatic pipes is rarely conducted in the past [4–7]. Most of the modelling research [4] was performed under various flow conditions on key flow phenomena. Some factors were not considered during modelling due to the limited understanding of mutual couplings between the gas and solid phases, such as carrier fluid turbulence modulation, gas–particle interactions, the relationship between the electrostatic force of particles and the air drag force etc. [8, 9]. Experimental research is not only able to obtain key parameters of particle flow under a variety of controllable flow conditions, but also provides actual boundary conditions for simulation study and useful information for validation of established models. However, most of the experimental research focused on the particles in circular-shaped pipes instead of the square-shaped ones. Besides, particle image velocimetry (PIV), phase-Doppler anemometry (PDA), fibre optic probe techniques, ray computed tomography, electrical capacitance tomography (ECT), microwave, acoustic and radioactive attenuation techniques have their limitations in the measurement of particle flow profile [1, 10–15].

In recent years, substantial efforts have been made to develop electrostatic techniques for the characterisation of particles in pneumatic pipes due to its advantages over other methods, including structural simplicity, robustness, low cost, etc. [6, 13, 16–19]. Whereas, little research has been conducted on the flow profiling of particles in square-shaped pipes [5]. Particle flow regimes [20] and electric field distribution of charged particles [7] in a square-shape pipe are more complex than those in a circular-shaped pipe. As the cross section of a square-shaped pipe is not centrosymmetric and has four right angles, small flow turbulence exists in the corner areas and particle distribution in the pipe cross section is very different from that of a ring-shaped pipe (especially the area near the pipe walls). A mathematical model of a square-shaped electrode was developed and its characteristics, including sensitivity distribution and frequency response, were theoretically analysed and experimentally verified by Murnane et al. [21] and Peng et al. [7]. The physical models of an intrusive rod electrode and distributed rod electrode for a large diameter rectangular pipe at the outlet of a coal mill were proposed by Jurjevčič et al. [3]. Mathematical modelling and experimental tests of non-intrusive strip-shaped electrostatic sensor arrays, which are uniformly embedded in the four pipe walls, for the measurement of pulverised fuel flow in a square-shaped pipe were conducted by Zhang et al. [6]. The experimental results have shown that the velocity profiles of air and particles over the whole cross-section of the pipe are similar and relatively non-uniform. However, parameters of particles in the centre of the pipe are deduced from those near the pipe walls. A large eddy simulation in a large range of high Reynolds numbers was conducted by Adams et al. [20] and its result demonstrates that the dynamic characteristics of particles close to the four sharp corners of the pipe are more complex than those in circular pipes. Therefore, an electrostatic sensing system that is capable of measuring the particle velocity and volumetric concentration profiles over the whole pipe cross section is desirable for the quantitative characterisation of pneumatically conveyed particles.

In this study, a sensor array composed of nine pairs of electrostatic electrodes is designed and implemented for measuring the volumetric concentration and velocity profiles of pneumatically conveyed particles in a square-shaped pipe. Experimental tests using plain flour as conveying material were conducted under various dilute phase flow conditions with combinations of different air velocities and mass flow rates. Concentration and velocity profiles of particles over a pipe cross section are obtained using localised particle flow parameters measured from the developed sensor array and a non-intrusive sensor array proposed by Zhang et al. [6]. A study on the mean volumetric concentration and velocity of particles over the whole cross section measured by these two different sensor arrays is also conducted.

2. Measurement principle and system design

2.1. Overall measurement strategy

The schematic block diagram of the measurement principles of the proposed electrostatic system is shown in Fig. 1. Particles are electrostatically charged when flowing through a pipe due to the collisions between particles, impacts between particles and pipe walls, and friction between particles and air. An electrostatic sensor head is embedded into the pipe of a gas–solid two-phase flow test rig to measure the electrostatic signals of pneumatically conveyed particles. The electric current signals from the electrostatic sensor arrays that embedded in the sensor head are converted into voltage signals and then amplified and filtered by a signal conditioning circuit [6, 22]. The filtered signals are sampled by a data acquisition card (DAQ) for the calculation of localised volumetric concentration and velocity of particles near the electrode. The signal processing algorithms and cross-correlation velocimetry are performed to obtain the local concentration and velocity of particles, respectively. The cross-sectional profiles (section 2.3) and cross-sectional mean particle concentration and velocity (section 2.4) are then obtained using the localised particle parameters.

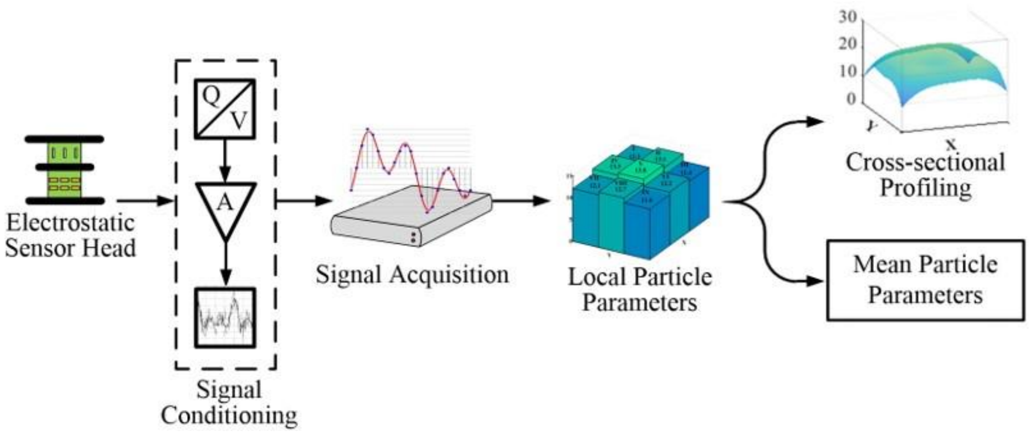

Fig. 1. Block diagram of the measurement system.

2.2. Design and implementation of electrostatic sensor head

Fig. 2 shows the structure of the proposed electrostatic sensor array (namely electrostatic sensor array 1) and the non-intrusive electrostatic sensor array designed by Zhang et al. [6] (namely electrostatic sensor array 2). Electrostatic sensor array 1 consists of nine pairs of strip-shaped electrostatic electrodes, which are inserted into the square-shaped pipe with an identical spacing in between. The surface of sensor array 1 (facing the flow) is made in the form of a knife-edge to minimise the flow disturbance. Electrostatic sensor array 2, which consists of 3×4 pairs of strip-shaped electrostatic electrodes that are uniformly embedded in the four flat pipe walls, is placed upstream of sensor array 1 to avoid the fluid disturbance caused by sensor array 1. Each electrode in the two sensor arrays has the same length and width, and the electrode spacing of each electrode pair is identical as well.

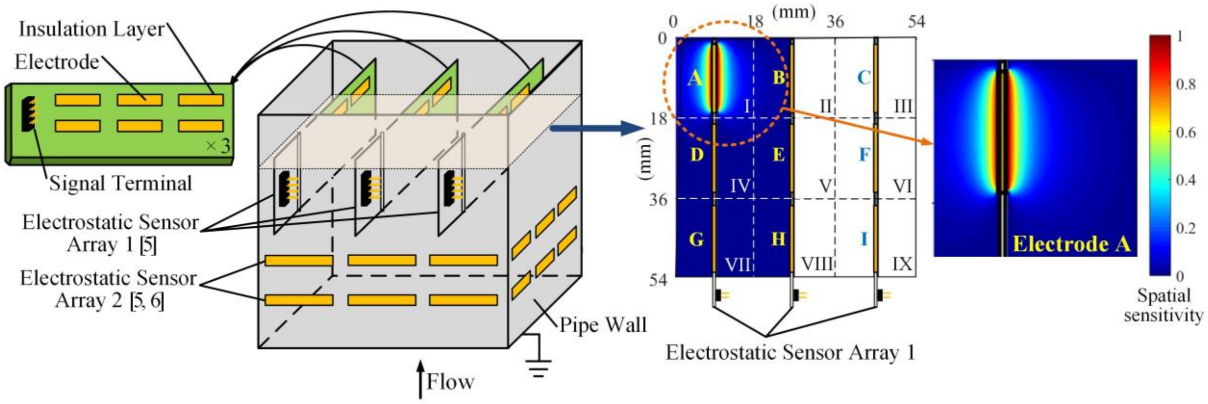

Fig. 2. Structure of the sensor head [5] and sensitivity distribution of electrostatic sensor array 1.

In order to determine the sensing characteristics of the sensor arrays, the spatial sensitivity of an individual strip-shaped electrode (marked as electrode A) within electrostatic sensor array 1 is simulated using the in-house software based on the finite element method (FEM) under the COMSOL Multiphysics environment. The simulation is validated using an analytical mathematical model (based on the theory of electrostatics and the method of images) proposed by Zhang et al. [6]. According to the dimensions of the sensor head used in the experimental work, the dimensions of the electrode (made of copper) used in the simulation has a length of 15 mm and a width of 3 mm, and the side-length of the pipe is set as 54 mm. The boundary conditions are set to ground for the electrode and zero charge for the outer surface of the model domain. As shown in Fig. 2, the sensitivity distribution of all electrodes of sensor array 1 can be derived by duplicate the sensitivity area of electrode A to other electrodes without regard to the interference between the adjacent electrodes as they are isolated by a grounding layer. As can be seen from Fig. 2, the sensitivity of the stripe-shaped electrode is not linear with the distance between the particles and the electrode. Electrostatic sensor array 1 is suitable for measured localised particle parameters as the strip-shaped electrode is more sensitive to its surrounding area. Because the strip-shaped electrode senses the particles on both of its left and right sides, it provides larger sensing volume and more uniform sensitivity than the similar electrodes used in reference [5]. Based upon the sensing area of each electrode, the square-shaped cross section is uniformly divided into nine measurement zones, i.e. Zones I, II, …, IX, as shown in Fig. 2, and one pair of electrodes are placed in the symmetry axis of each zone. The number of electrodes is a trade-off between the intrusive effect of the electrodes and the spatial resolution of the sensor. Because if this number is too large, a more detailed measurement of local particle parameters can be obtained, while the movement of the particle flows in the pipe will be hindered by the intrusive electrodes. Besides, a powerful computer with high calculation speed is required due to heavy computation. On the contrary, if the number is too small, the profiles of particle flow parameters cannot be obtained with sufficient details and the mean particle concentration and velocity cannot be calculated using less localised particle parameters measured over the pipe cross section.

The degree of the intrusiveness of electrostatic sensor array 1 depends mainly on the sensor configuration, such as the dimensions and spacing of the electrodes. To mitigate the intrusive effect of electrostatic sensor array 1 on pneumatically conveyed particles, the thickness of the sensor array is made to be 0.6 mm in the experiment so that only 3.3% of the pipe cross section is occupied by the sensor array. Furthermore, the wind-facing side of the sensor array is made as a sharp corner of 60° to weaken the flow turbulence and vortex caused by the blockage and to minimise the chance of collision with particles. As the volumetric concentration of particles is normally as low as 0.1% in fully suspension conditions, only a tiny proportion of particles will collide with the electrodes. Therefore, minimum effect on the movement behaviours of particles can be achieved by the sensor design and the moving trajectory of most particles still follows the conveying air. As can be seen from Fig. 3, the insertion of sensor array 1 has limited effect on the air flow field in the sensing area of the electrodes. As the air velocity in wind-facing area (green and yellow coloured area) of the sensor array is a bit lower than the preset air velocity (27 m/s), the upstream electrode is located about 6 mm from the sensor edge to avoid the flow turbulence. A few small eddy currents only appear in the downstream area of the sensor array, therefore, have very limited effects on the air velocity near the downstream electrode.

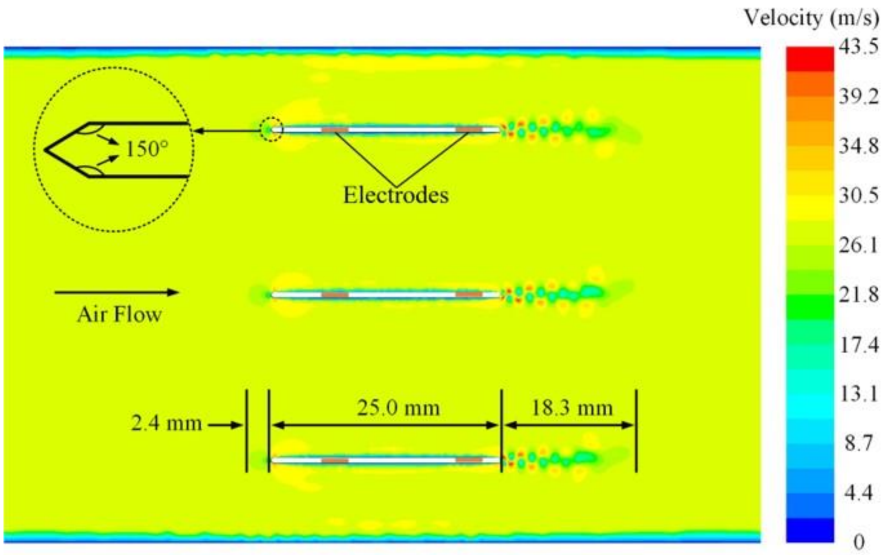

Fig. 3. Velocity distribution of air flow with the presence of electrostatic sensor array 1.

Fig. 4 shows the implemented electrostatic sensor head consisting of the electrostatic sensor arrays 1 and 2 according to the design presented in section 2. Sensor array 1 is located about 10 cm downstream to sensor array 2 and inserted into the square-shaped pipe through three rectangular grooves on one side of the pipe wall to obtain local particle flow information directly. Polymethyl methacrylate is utilised as the main body of sensor array 1 due to the advantage of easy machining. The whole sensor head is covered by a grounded shielding case to isolate both sensor arrays from external electromagnetic interference. As can be seen from Fig. 4, three holes on the upper side of the grooves are used for inserting a hot-wire anemometer (Model MP210, KIMO, France) to measure air velocity prior to each particle flow test. The pure air velocities in the nine zones of the pipe cross section are measured for the purpose of comparison with those in the presence of particles. The twelve pairs of strip-shaped electrostatic electrodes within sensor array 2 are uniformly embedded in the four flat pipe walls to obtain local particle flow information using the weighting method presented by Zhang et al. [6]. As shown in Fig. 4, nine pairs of strip-shaped electrodes embedded in three identical printed circuit boards (PCBs) are inserted to the square-shaped pipe. Each electrode (silver coloured) has a length of 15 mm and a width of 3 mm, and the spacings between two lateral electrodes are 18 mm and 15 mm, respectively. All the electrodes are physically separated from each other using a very thin insulation layer and electrically isolated by a grounded metal layer (green area). The signal from an electrostatic electrode is amplified and filtered before being sampled for flow parameter calculation since the raw signal is very weak and can be easily distorted by environmental interferes. Fig. 4 also shows the signal conditioning circuit board consisting of three modules, i.e. power supply voltage regulation, signal amplification, and signal filtering modules. The cut-off frequency of the low-pass filter circuit is set to about 16 kHz to retain the useful signal. A grounding shield is utilised to prevent the measured signal from external environmental interference by covering the electronic components on the signal conditioning circuit board. The Bayonet Nut Connector (BNC) and mini USB connectors are used for the connection to an electrode and the conditioned signal transmission to the signal acquisition unit, respectively.

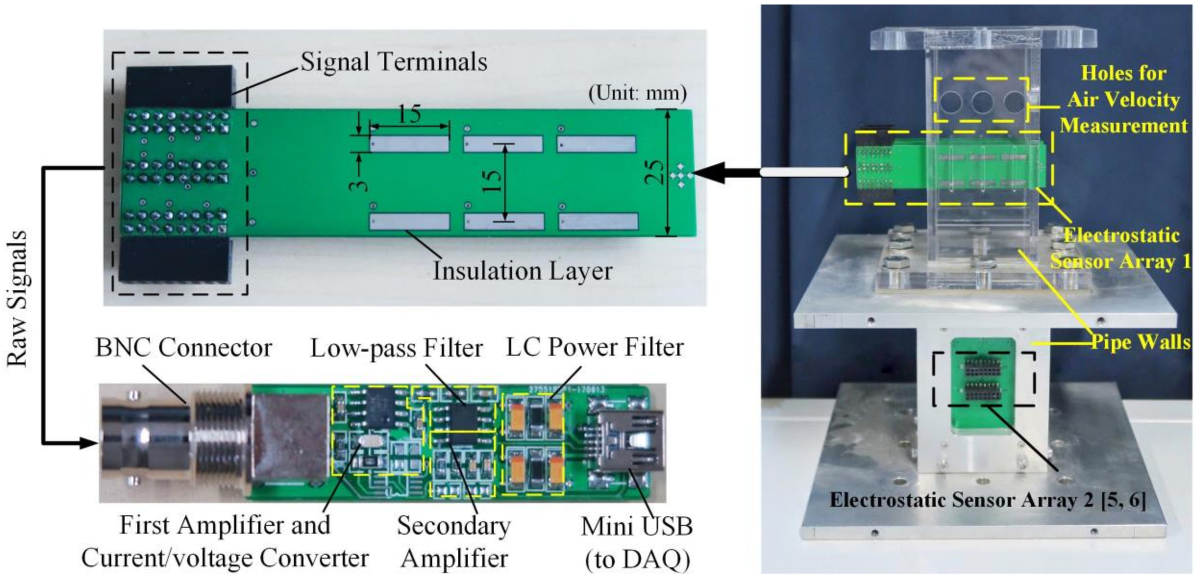

Fig. 4. Implementation of the sensor head and signal conditioning circuit board.

2.3. Cross-sectional profiling of particles

The signals from the electrodes mounted inside the pipe contain dynamic information of local particles. Sensing Zones I, II, …, IX in Fig. 2 are represented by i = 1, 2, …, 9, respectively. The relative volumetric concentration of local particles (β_i, hereafter referred to as particle concentration) in one zone is represented by the root-mean-square (RMS) value of measured electrostatic signals (A_{RMS}) [3, 6, 13, 18 , 20–24] and local particle velocity (v_i) is calculated through cross-correlation velocimetry [6, 7, 13, 17, 18, 19, 22, 25]. According to the spatial sensitivity distributions of both electrostatic sensor arrays 1 and 2, the electrostatic signals from sensor array 1 contain information about the particles over the whole pipe cross section, while those from sensor array 2 contain information about the particle flow near the pipe walls [6]. In order to obtain an in-depth understanding of the particle flow dynamics over the pipe cross section, the relative concentration and velocity profiles of particle flow are obtained using the biharmonic spline interpolation method [26, 27] other than a simple combination of the particle parameters measured in each of the nine zones [5]. Biharmonic spline interpolation, also known as biharmonic spline filtering, is a solution to the biharmonic equation based on the Green's function [26–28], which is initially developed to solve elasticity problems, such as calculate the elastic force distribution of a curved stretchable surface based on the mean elastic forces of several discrete small areas. Obtained data points are smoothly connected in this way, which illustrated that this method is superior to other interpolation methods, such as linear method, cubic method, nearest neighbour method etc. In this study, the pipe cross section is divided into a number of small areas and the volumetric concentration and velocity of particles in several specific areas can be measured with both sensor arrays. All the particles are subjected to the resultant force due to air drag, gravity, etc. Therefore, the concentration and velocity distribution of particles in the pipe cross section can be obtained using biharmonic spline interpolation method. The values of measured parameters of local particles (located at x_1, x_2, …, x_N) using all the electrostatic sensors over the cross section (with the number of N) are $\alpha(x_1)$, $\alpha(x_2)$, …, $\alpha(x_N)$, respectively. The position of one small area (x) and the displacement of the interpolation surface at x ($\alpha(x)$) satisfy biharmonic equation [26]:

$$\nabla^4 \alpha(x) = \sum_{j=1}^{N} \omega_j \delta(x - x_j) \tag{1}$$

where ∇^4 is the Biharmonic operator, $\delta(x)$ is Delta Function, j is the serial numbers of the measuring points (j=1, 2, …, N) and ω_j is a weighting coefficient to represent the magnitude of the resultant force. The particular solution to Eq. (1) can be expressed as the following linear combination of 2-dimensional Green's functions ($g_2(x\text{-}x_j)$):

$$\alpha(x) = \sum_{j=1}^{N} \omega_j g_2(x - x_j) \tag{2}$$

where the weight coefficient (ω_j) can be obtained by solving the following linear equation since x_i and $\alpha(x_i)$ are known (i=1, 2, …, N):

$$\alpha(x_i) = \sum_{j=1}^{N} \omega_j g_2(x_i - x_j) \tag{3}$$

Consequently, the displacement of the interpolation surface ($\alpha(x)$) at each area position (x) can be calculated using Eq. (2) and the interpolation surface can be plotted.

2.4. Cross-sectional mean parameters of particles

The mean volumetric concentration ($\bar{\beta}$) and velocity ($\bar{v}$) of particles over the whole pipe cross section are also concerned in the characterisation of particle flow. The mean particle parameters and their evaluation parameters, i.e. the maximum difference of particle concentrations and velocities and their normalised values, are calculated through this approach (using the particle flow parameters from both sensor arrays) to analyse the characteristics of particle flows over the whole pipe cross section quantitatively. The mean particle concentration can be obtained as follows:

$$\bar{\beta} = \frac{S_p}{S} = \frac{\sum_{i=1}^{9} \beta_i S_i}{\sum_{i=1}^{9} S_i} = \frac{\sum_{i=1}^{9} \beta_i}{9} \tag{4}$$

where S_p is the total cross-sectional area occupied by the particles, S is the pipe cross-sectional area and S_i is the area of one zone over the pipe cross section. Since the particle distribution over the pipe cross section is non-uniform, local particle concentration is employed as a weighting factor in mean particle velocity calculation [25].

$$\bar{v} = \frac{q_v}{S_p} = \frac{\sum_{i=1}^{9} v_i \beta_i S_i}{\sum_{i=1}^{9} \beta_i S_i} = \frac{\sum_{i=1}^{9} v_i \beta_i}{\sum_{i=1}^{9} \beta_i} \tag{5}$$

where q_v is the volumetric flow rate of particles.

To characterise the variation range of the particle concentration and velocity profiles, the maximum difference of particle concentrations (d_β) and velocities (d_v) over the whole pipe cross section are calculated through the following equations:

$$d_\beta = \max(\sum_{i=1}^{9} \beta_i) - \min(\sum_{i=1}^{9} \beta_i) \tag{6}$$

$$d_v = \max(\sum_{i=1}^{9} v_i) - \min(\sum_{i=1}^{9} v_i) \tag{7}$$

Since d_β and d_v are concerned with $\bar{\beta}$ and $\bar{v}$, respectively, the normalised maximum difference of particle concentrations (D_β) and velocities (D_v) can be obtained as follows:

$$D_\beta = \frac{d_\beta}{\bar{\beta}} \times 100\% \tag{8}$$

$$D_v = \frac{d_v}{\bar{v}} \times 100\% \tag{9}$$

3. Experimental results and discussion

3.1. Test rig and experimental conditions

A laboratory scale carbon steel test rig with a square-shaped pneumatic conveying pipe, as shown in Fig. 5, was used in the experimental tests. The dimension of the inner pipe wall is 54 mm×54 mm. A negative pressure generating device with a receiving hopper for particle recycling is used to create different air velocities for the pneumatic conveying of particles. A double-screw feeder with a programmable controller is employed to provide a stable particle flow rate during each test. The pipe walls close to and far from the readers are marked as sides X and X', respectively. While the pipe walls close to the medial and lateral walls of the right lower bend of the rig are marked as sides Y and Y', respectively. Experimental tests were conducted on vertical and horizontal pipe sections using plain flour as conveying material under the laboratory environment. Plain flour is used as conveying material in the tests because it is a representative of fine particles that widely exist in many industries.

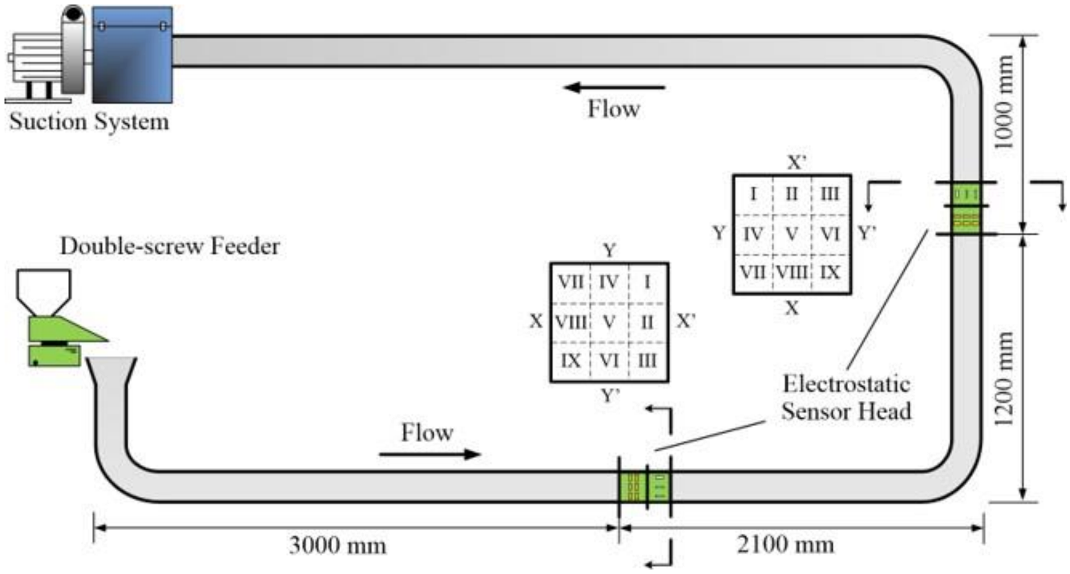

Fig. 5. Layout of particle flow test rig with a square-shaped pipe.

The particle size distribution of plain flour, as shown in Fig. 6, was measured using a laser particle size analyser (Model LOP9, OMEC, China). As can be seen from Fig. 6, the median diameter (D50) of plain flour used in the tests is 61.83 μm and the most populated particles (14.6 percent, vertical axis Y) are within the range from 98 to 124 μm (horizontal axis X). Such parameters are similar to pulverised coal used in coal-fired power plants, medicinal powder in the pharmaceutical industry and various chemical compound particles in the chemical industry.

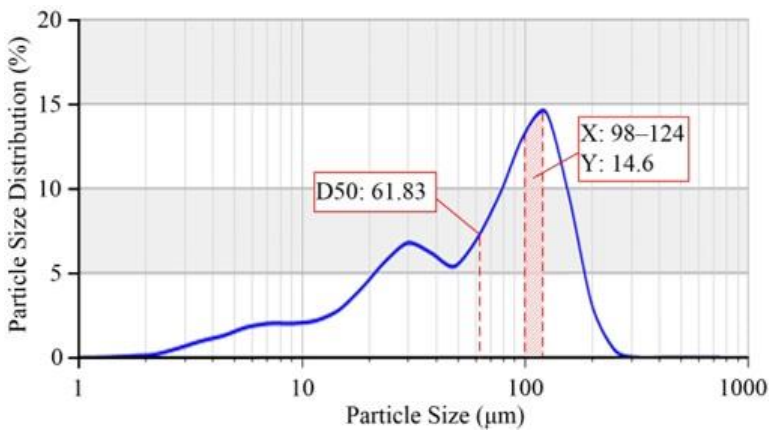

Fig. 6. Particle size distribution of plain flour particles.

All the tests were conducted under an air conditioning environment with an ambient temperature of 26.1 ℃, the relative humidity of 69% and the ambient PM2.5 (particulate matter that has a diameter of less than 2.5 μm) density of 62 μg/m3. As shown in Table 1, experimental tests were conducted under sixteen test conditions, i.e. combinations of four air velocities (measured in Zone V) and four mass flow rates. The equivalent particle volumetric concentrations under different test conditions were within the range from about 0.0012% to 0.0077%. In order to avoid the air velocity drop caused by the negative pressure generating device during long operation period, the air velocity in the central zone of the pipe was calibrated using the hot-wire anemometer before each test. During each test, the electrostatic signals from both electrostatic sensor arrays 1 and 2 were conditioned by the same signal conditioning circuit board aforementioned, sampled synchronously by a data acquisition card (Model USB-6363, National Instruments) and then processed by a host computer when the particle flow has reached a relatively stable state.

Table 1 Test matrix of plain flour

Mass flow rate (kg/h)	Air velocity (m/s)			
	V1=19	V2=23	V3=27	V4=31
M1=2	V1M1	V2M1	V3M1	V4M1
M2=4	V1M2	V2M2	V3M2	V4M2
M3=6	V1M3	V2M3	V3M3	V4M3
M4=8	V1M4	V2M4	V3M4	V4M4

The particle flow is regarded as stable when all the pipes are filled with particles, the test rig is running normally and the RMS value of measured signal fluctuates in a small range. The signal sampling frequency is set at 25 kHz and 2048 data points are used to calculate particle concentration and velocity in each measurement cycle. A total of 240 concentration and velocity readings were obtained, at least, from each pair of electrodes under each test condition to derive particle flow parameter in each zone.

3.2. Features of electrostatic signals

The features of the electrostatic signals measured by different electrode pairs reflect the dynamic behaviours of particles in the corresponding measurement zones across the whole pipe cross section. The simultaneously sampled raw electrostatic signals of particles from the upstream and downstream electrodes in Zones I, II III and V of the horizontal pipe under V3=27 m/s, M2=4 kg/h condition are shown in Fig. 7. The mean absolute value of the signals measured in the upper corner zone (Zone I) is 0.43, which is the smallest. The mean absolute value of the signals in the zone (Zone II) is lower than that in the lowest corner zone (Zone III). In addition, the mean absolute value of the signals in the central zone (Zone V) is higher than that in the zone with one side pipe wall adjacent at the same height (Zone II). To analyse the raw signals shown in Fig. 7 further, the corresponding power spectral densities (PSDs) are plotted in Fig. 8 to illustrate the frequency-domain features of the signals. As can be seen from Fig. 8, it is evident that the main peak frequencies of the electrostatic signals in the four zones vary from 561.5 Hz to 732.4 Hz (illustrated by the vertical dash lines). The area surrounded by the PSD curve represents the magnitude of the signal energy, which reflects particle concentration, velocity etc. It is noticeable that the signal energy of moving particles in the bottom zone (Zone III) is the highest as more particles are transported on the bottom of the pipe due to the gravitational effect. On the contrary, the signal energy of particles in the upper corner zone (Zone I) is the lowest, which agrees well with the trend in the amplitude of raw electrostatic signals shown in Fig. 7. The signal energy of particles in the central zone (Zone V) is slightly higher than that in the adjacent zone because fewer particles travel slower in Zone II due to the impact between particles and pipe wall.

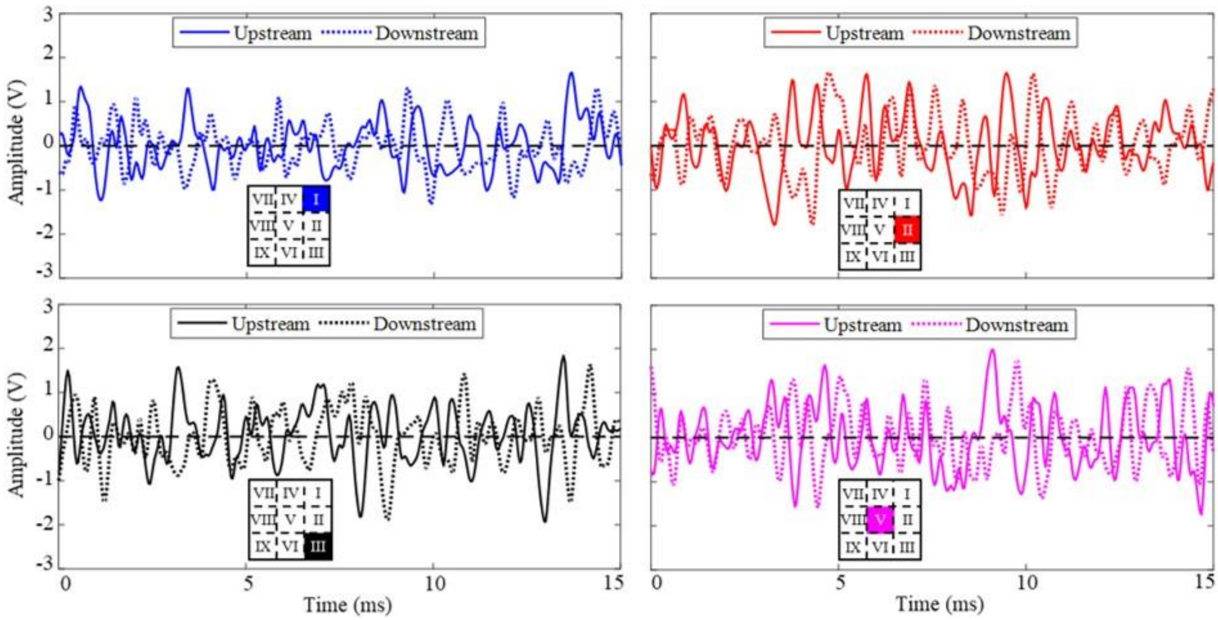

Fig. 7. Raw electrostatic signals of particles in Zones I, II, III and V of the horizontal pipe.

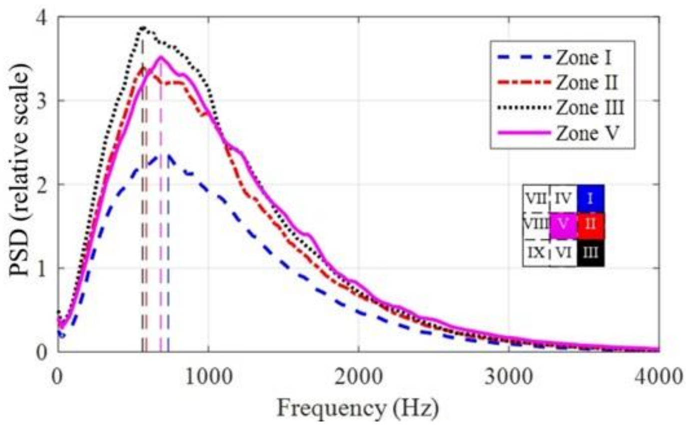

Fig. 8. PSDs of electrostatic signals of particles in Zones I, II, III and V of the horizontal pipe.

3.3. Cross-sectional profiling of particle concentration and velocity

Fig. 9 shows the RMS charge levels of the electrostatic signals (as an evaluation of particle relative concentration) measured in the cross sections of both horizontal and vertical pipes under all test conditions measured by electrostatic sensor array 1. The cross-sectional concentration profiles of particle flow are obtained using the biharmonic spline interpolation method based on the measurement results from both electrostatic sensor arrays 1 and 2, as shown in Fig. 10. It is clear that the profiles are able to provide qualitative images of the particle concentration in the pipe cross section. As can be seen from Figs. 9 and 10, the RMS charge level of the signal increases with the mass flow rate since more particles are fed into the pipe while the air velocity is unchanged. The RMS charge level decreases slightly with the increasing air velocity when the mass flow rate keeps constant because the particle concentration slightly decreases at a higher air velocity. This result demonstrates that the RMS charge level of the signal is basically insusceptible to the air velocity, which indicates that the RMS charge level of the signal can be regarded as relative particle concentration in the same flow condition. The concentrations of particles in different zones are non-uniform over the whole pipe cross section. In horizontal pipe sections, more particles are transported at the bottom of the pipe (Zone III, VI and IX) than those at the top of the pipe (Zones I, IV and VII) mainly due to the gravitational effect. Besides, the particle concentration in the central zone (Zone V) is slightly higher than the zones of the same height with one side pipe wall adjacent to it (Zones II and VIII), which agrees with the trend in Fig. 7 and 8. As shown in Fig. 9, the slopes of three lines that through the points of Zones I, II, III, Zones IV, V, VI and Zones VII, VIII, IX decrease as the particle velocity increases. In other words, particles concentrations in zones with the same horizontal position and different heights are getting closer at a higher particle velocity, which means a more even particle concentration distribution. In vertical pipe sections, the particle concentrations in four zones (Zones II, IV, VI, and VIII) adjacent to the central zone are lower compared with those in four corner zones (Zones I, III, VII and IX) and the lowest particle concentration is measured in the central zone (Zone V). When the particles flow from the horizontal pipe section to the vertical pipe section through a bend, the slope-shaped particle concentration profile changes to an arch-shaped one.

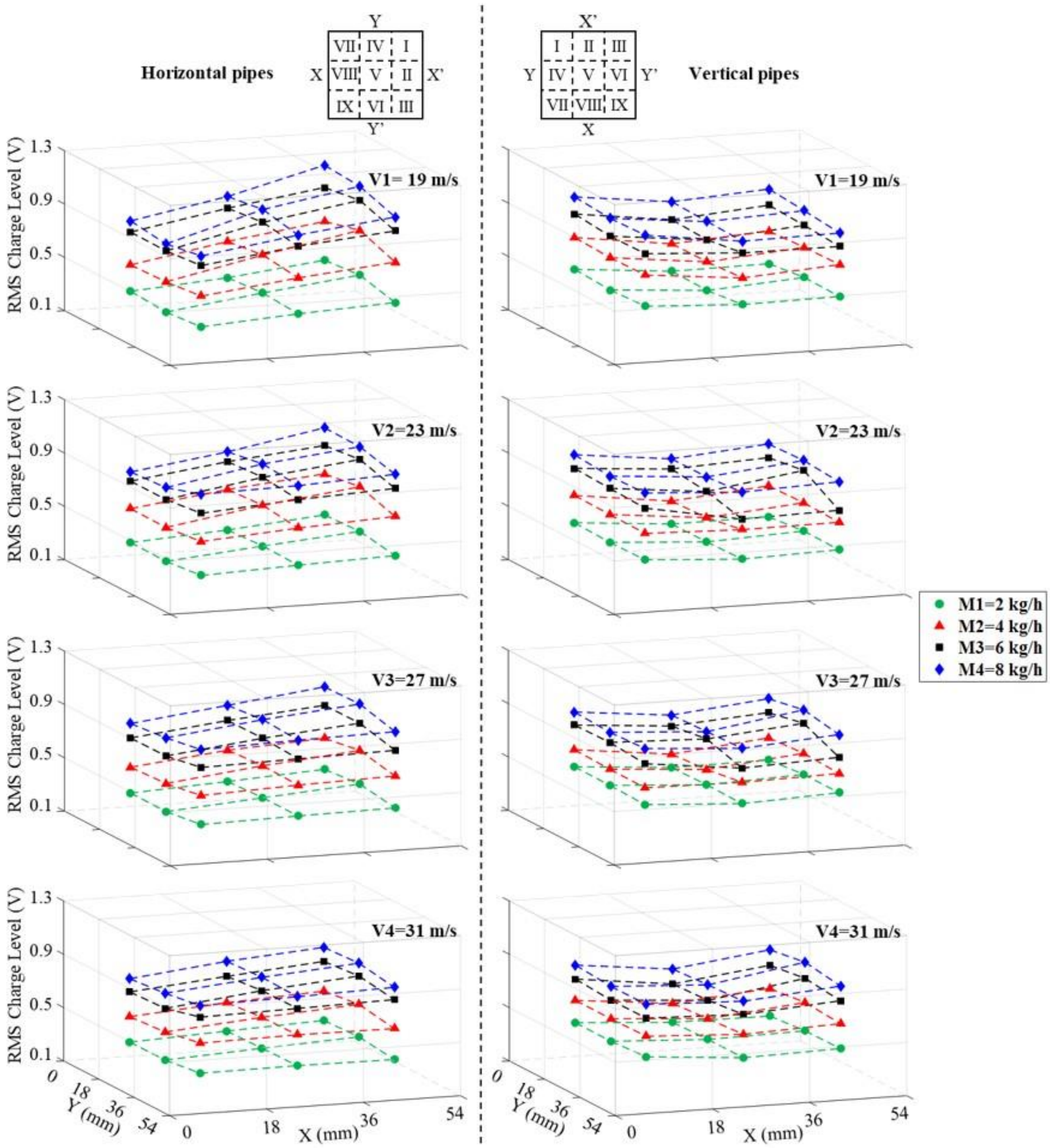

Fig. 9. Particle concentration distribution under different particle mass flow rate and air velocity conditions.

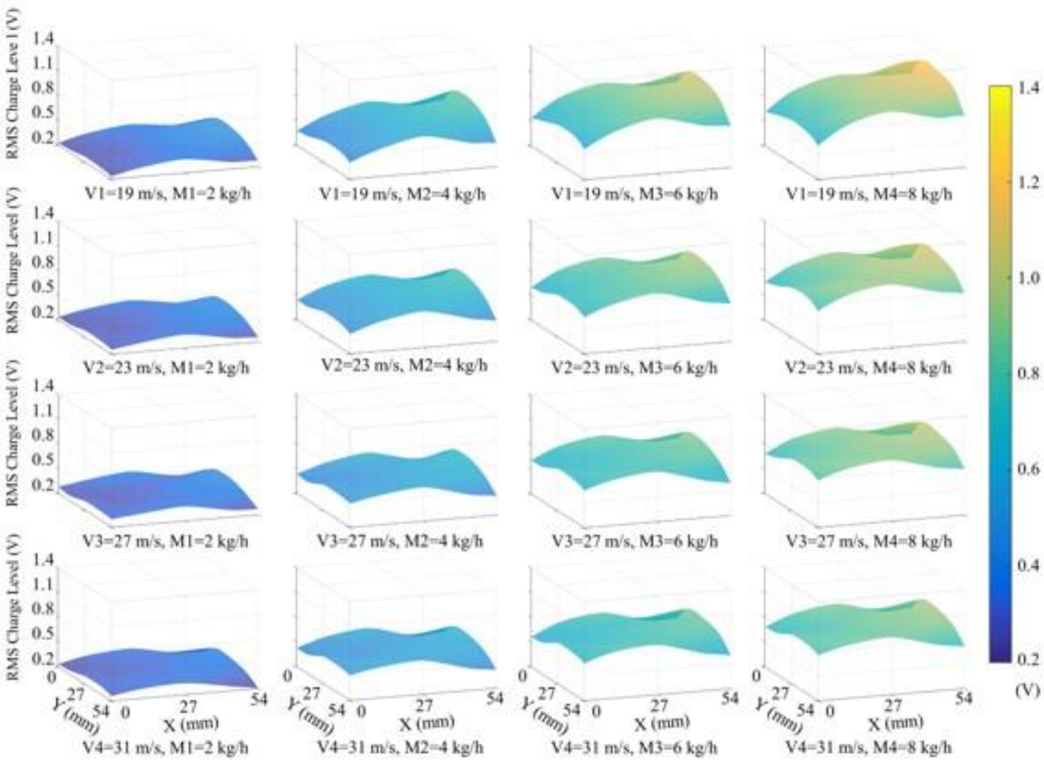

(a)

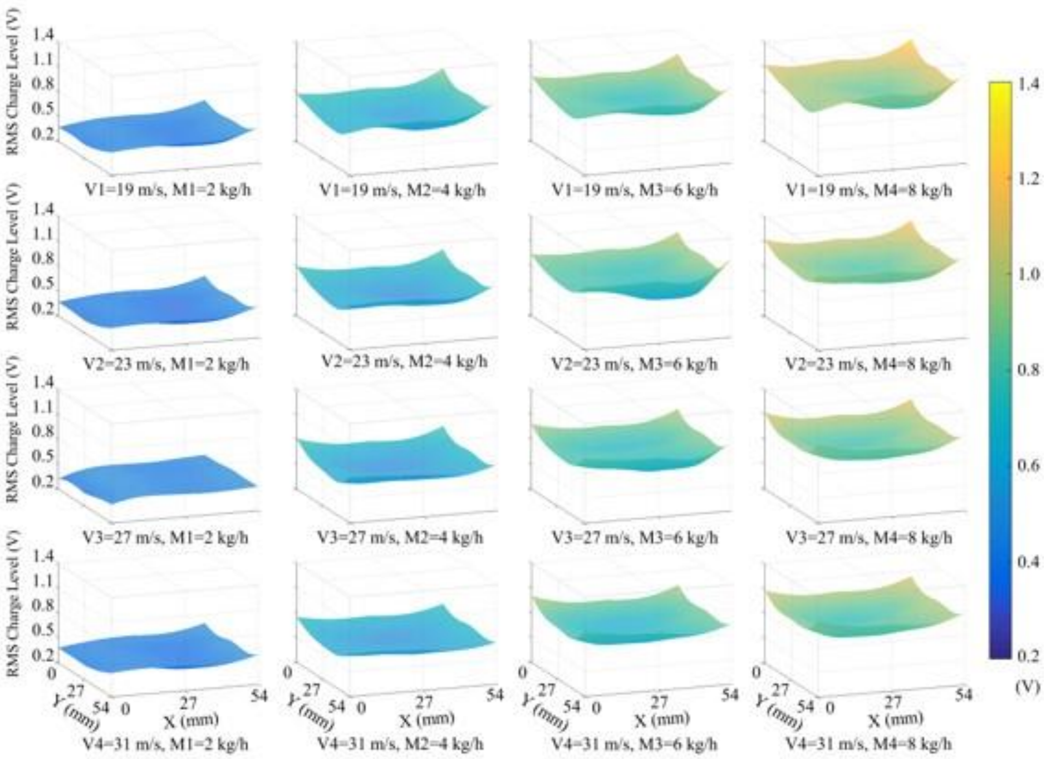

(b)

Fig. 10. Particle concentration profiles under different particle mass flow rate and air velocity conditions: (a) horizontal pipe; (b) vertical pipe.

The velocity distributions of pure air flow and particles under different test conditions are shown in Fig. 11. As can be seen from Fig. 11, the velocity distributions of both pure air and particles are not uniform in the cross sections of horizontal and vertical pipes but have very similar variation trends under different flow conditions. The velocity of the air in the central zone (Zone V) is the highest. The air velocities in the four zones (Zones II, IV, VI, and VIII) adjacent to the central zone are higher than those in four corner zones (Zones I, III, VII, and IX). In the horizontal pipe, it is noticeable that the air velocities in the top zones (Zones I, IV and VII) are similar to those in the bottom zones (Zones III, VI and IX). In the vertical pipe, the air in three zones close to the pipe wall Y (Zones I, IV, and VII) travel slower than those in three zones close to the pipe wall Y' (Zones III, VI, and IX). This tendency demonstrates that the velocity distribution of air is still asymmetric in the measurement pipe section, although the sensor head is placed 20 times of the pipe inner dimension away from the upstream bend to avoid the effect of the centrifugal force. In general, the particle velocity distributions under the four different air velocities agree with the trend in air velocity profiles, but with different distribution compare to the particle concentration distribution. The particle velocity profiles based on the measurement results from electrostatic sensor arrays 1 and 2 are shown in Fig. 12. As can be seen from Figs. 11 and 12, the particle velocities in all zones increase with the conveying air velocities correspondingly due to the larger air drag force. When the air velocity remains unchanged, the velocity difference between the particles and the conveying air (slip velocity) increases with the mass flow rate because the presence of particles has an obstructive effect on the air flow (Fig. 11). Besides, the slip velocity in the vertical pipe is higher than that in the horizontal pipe under the same test condition due to gravity. However, in horizontal pipe sections, the velocities of the particles in the top zones (Zones I, IV and VII) are higher than those in the bottom zones (Zones III, VI and IX), which is inconsistent with the air velocity distribution (Fig. 11). Due to more particles need to be conveyed in the bottom zones because of gravity, the viscous force applied to the air flows is stronger, and hence, particle velocities in the bottom zones is lower.

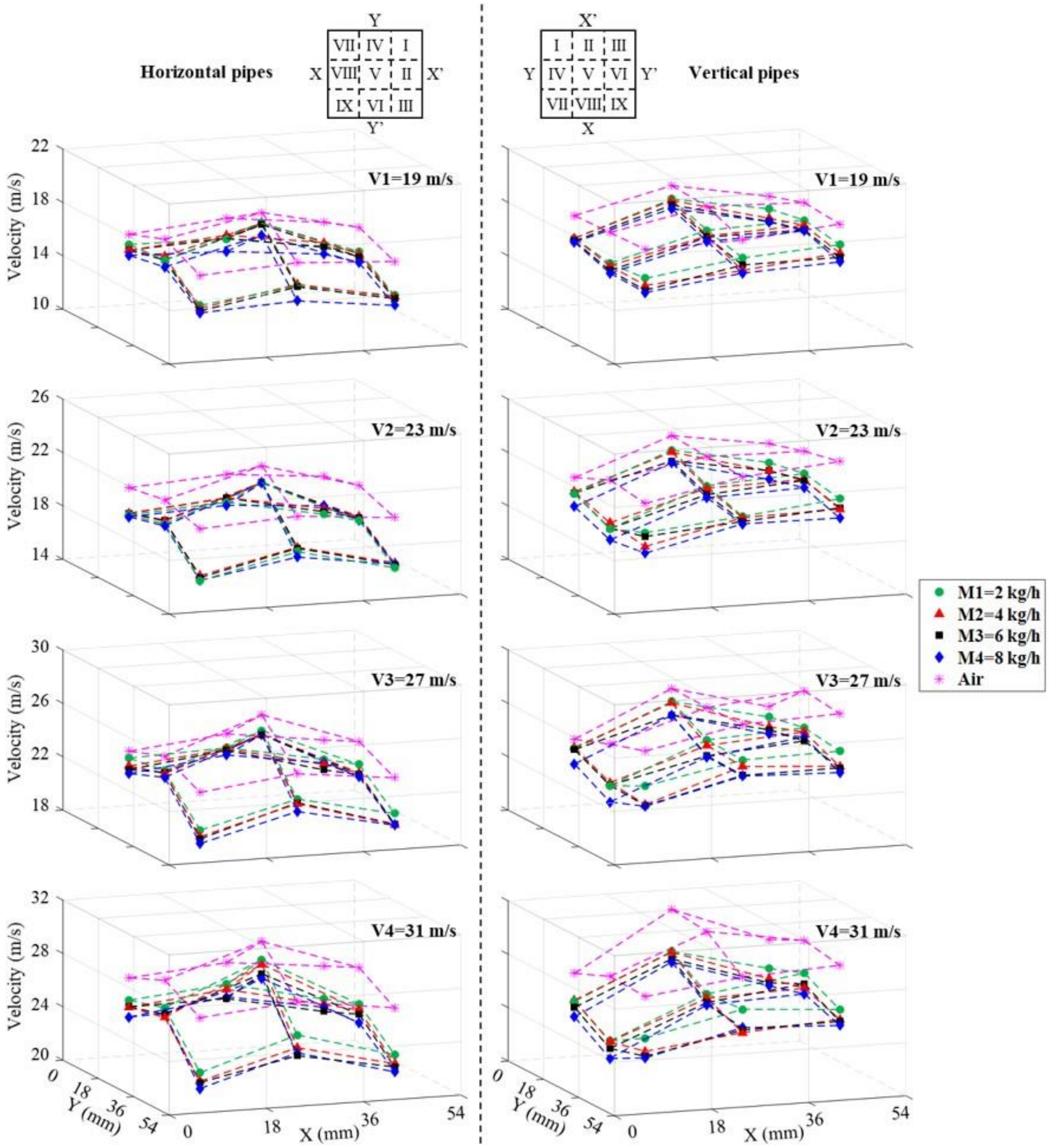

Fig. 11. Particle velocity distribution under different particle mass flow rate and air velocity conditions.

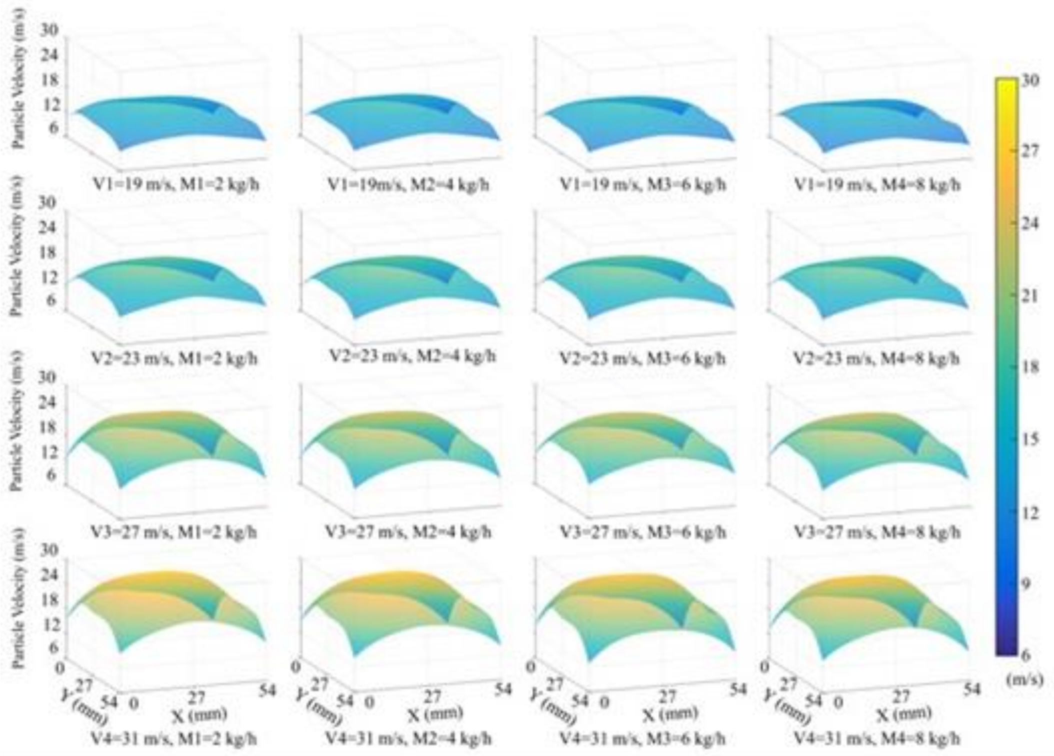

(a)

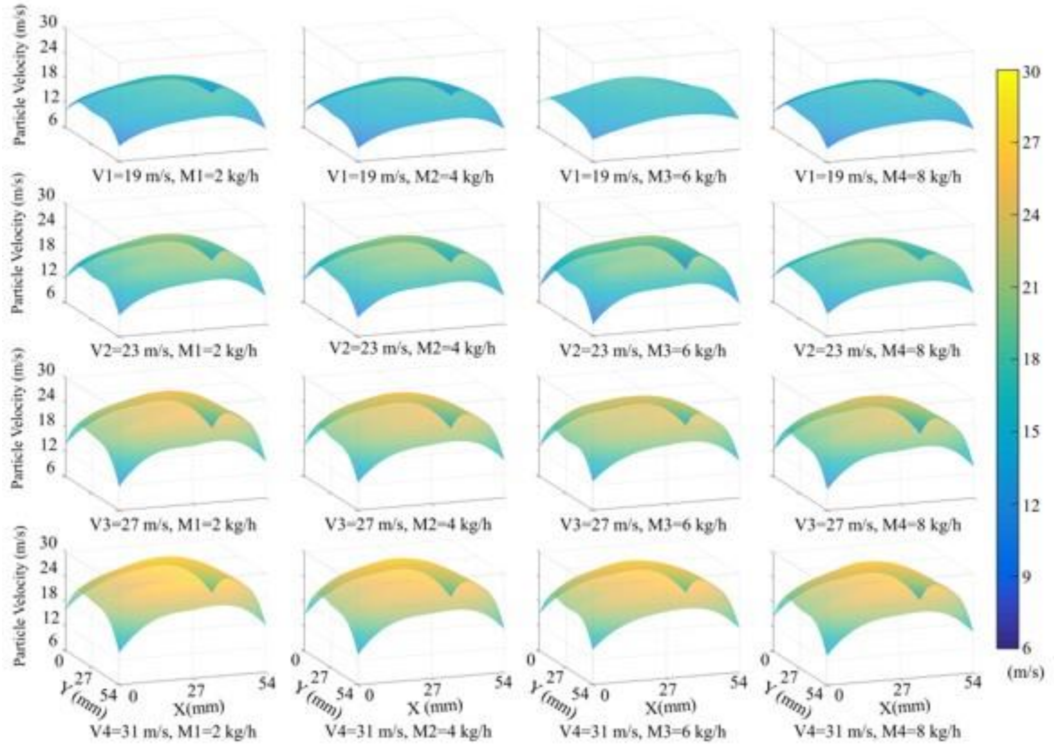

(b)

Fig. 12. Particle velocity profiles under different particle mass flow rate and air velocity conditions: (a) horizontal pipe; (b) vertical pipe.

3.4. Cross-sectional mean particle velocities and concentrations

The cross-sectional mean volumetric concentration and velocity of particles are common characteristics for industry processes monitoring. Therefore, a study on the mean particle cross-sectional parameters (Eq. (4)

and (5)) over the pipe measured by electrostatic sensor arrays 1 and 2, respectively, were conducted. Mean particle concentrations measured by these two sensor arrays under sixteen test conditions (as shown in Table 1) are shown in Fig. 13. As can be seen from Fig. 13, the variation trends of the mean particle concentrations measured by both of the sensor arrays are similar. The mean RMS charge level of the signals increases about 0.18 V on average for every 2.0 kg/h increase in particle mass flow rate when the air velocity remains unchanged. The mean RMS charge level of the signals decreases by 0.02 V with every 4 m/s increase of air velocity. In addition, the standard deviation of RMS charge level increases by 0.01 V on average for every 2 kg/h increase in particle mass flow rate and decreases by 0.01 V for every 4 m/s increase in air velocity, which is consistent with the RMS charge level. The mean RMS charge levels of the signals measured by the two sensor arrays have obvious gaps but with similar trends when plain flour particles flow from the horizontal pipe section to the vertical pipe section. The mean RMS charge level of the signals measured by sensor array 1 increases 0.01 V, while that measured by sensor array 2 increases 0.12 V, which is much higher than that derived from sensor array 1. Because there are fewer particles in the pipe centre than those near the pipe walls (Fig. 11) in the vertical pipe.

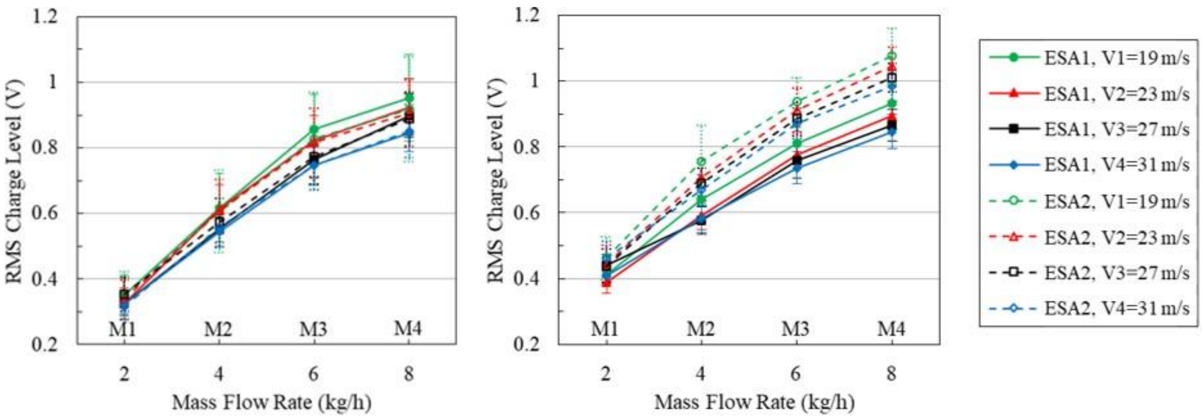

(a) (b)

Fig. 13. Mean RMS charge levels measured by electrostatic sensor array 1 (ESA1) and electrostatic sensor array 2 (ESA2) under different test conditions: (a) horizontal pipe; (b) vertical pipe.

The normalised maximum differences of RMS charge levels of the signals measured by electrostatic sensor arrays 1 and 2 are plotted in Fig. 14. A greater normalised maximum difference of RMS charge levels of the signals means a larger slope of particle concentration profile in a horizontal pipe considering the variation of the mean particle velocities. While a greater normalised maximum difference means a higher height of the arch of the normalised particle concentration profile in a vertical pipe. As can be seen from Fig. 14, the normalised maximum differences measured by sensor array 1 are 5.4% smaller than those by sensor array 2 on average under the same test conditions on average. The normalised maximum differences measured in the vertical pipe are 14.0% less than those measured in the horizontal pipe in the same test conditions on average due to the gravitational effect. In addition, the normalised maximum difference reduces by 4.5% for every 2 kg/h increase in particle mass flow rate and reduces by 4.6% for every 4 m/s increase in air velocity. Such a phenomenon is probably due to the larger viscous force applied to the air flows and the higher collision probability between particles and, consequently, the normalised curvatures of the concentration profiles tend to be smaller.

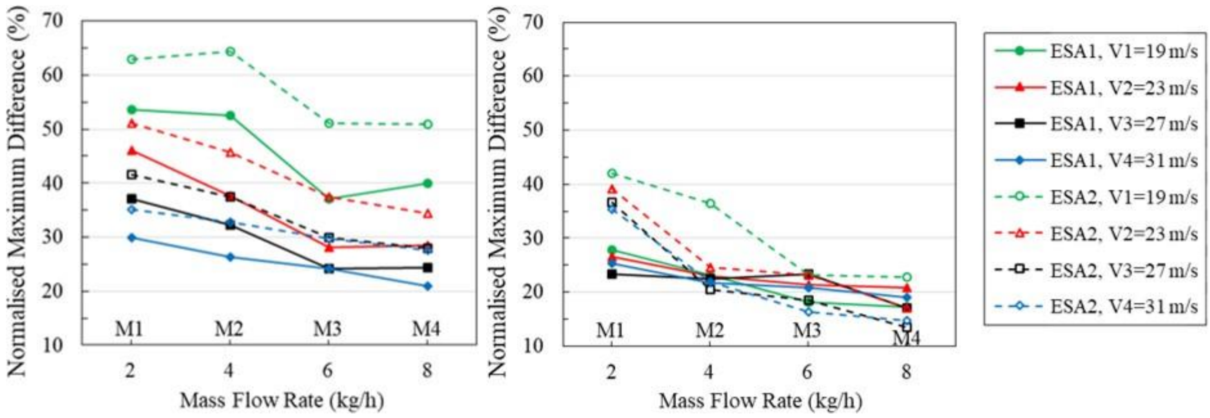

Fig. 14. Normalised maximum differences of RMS charge levels of the signals measured by electrostatic sensor array 1 and electrostatic sensor array 2 under different test conditions: (a) horizontal pipe; (b) vertical pipe.

The cross-sectional mean particle velocities under sixteen test conditions are shown in Fig. 15. As can be seen from Fig. 15, the mean particle velocity increases 2.8 m/s on average for every 4 m/s increase in the air velocity when the particle mass flow rate is fixed. The mean particle velocity decreases by 0.3 m/s with every 2.0 kg/h increment of particle mass flow rate because of the limitation of the drag force of conveying air. Besides, the standard deviation of it increases by 0.19 m/s on average for every 4 m/s increase in air velocity and keeps unchanged with the increasing particle mass flow rate. Under the same test condition, the mean particle velocities measured by electrostatic sensor array 1 are 3.2 m/s higher on average than those measured by electrostatic sensor array 2, and their difference increases 0.6 m/s for every 4 m/s increase in air velocity. Because the velocity of the particles in the central area of pipe cross section is higher than that near the pipe walls (Fig. 12) and sensor array 1 is more sensitive to the particles in the whole pipe cross section compared to sensor array 2. The mean particle velocities in the vertical pipe section are 1.7 m/s higher on average than those in the horizontal pipe section since the vertical pipe section is closer to the suction system.

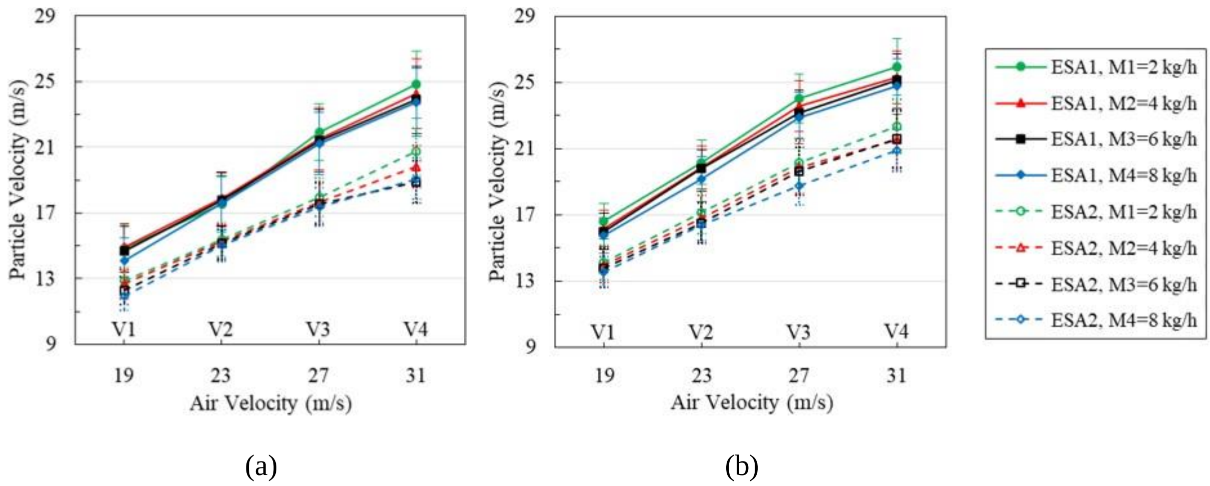

Fig. 15. Mean particle velocities measured by electrostatic sensor array 1 and electrostatic sensor array 2 under different test conditions: (a) horizontal pipe; (b) vertical pipe.

The normalised maximum differences of velocities measured by electrostatic sensor arrays 1 and 2 are plotted in Fig. 16 to illustrate the overall velocity profiles across the pipe. A greater normalised maximum difference of velocities means a higher arch of the normalised particle velocity profile. As can be seen from Fig. 16, the normalised maximum differences remain constant with the increasing conveying air velocity or particle mass flow rate, which is inconsistent with the trend of the normalised maximum differences of RMS charge levels of the signals (Fig. 14). In the horizontal pipe, the normalised maximum differences measured by sensor array 1 are 8.1% higher than those by sensor array 2 on average under the same test conditions due to the difference of sensing areas of the two sensor arrays. Additionally, the normalised maximum differences measured by sensor array 1 in the vertical pipe are 8.9% less than those measured in the horizontal pipe in the same test conditions on average due to the gravitational effect. However, the normalised maximum differences measured by sensor array 2 in horizontal and vertical pipes are similar. Because the particle velocity in the central zone is obtained from the weighting method and the same weight coefficient is used for both horizontal and vertical pipe tests. As illustrated in Fig. 12, the maximum particle velocities are measured in the pipe centre and the minimum velocities are measured near the pipe walls. Consequently, the normalised maximum differences measured by sensor array 2 change very little. This result demonstrates that the measurement accuracy of the sensor array 2 is essentially affected by the choice of weighting coefficient, indicating that sensor array 1 is more reliable than sensor array 2 when measuring the local parameters inside the pipe. Therefore, the developed electrostatic sensor array can be used to calibrate other types of non-intrusive ones for flow parameter measurement in a square-shaped pipe.

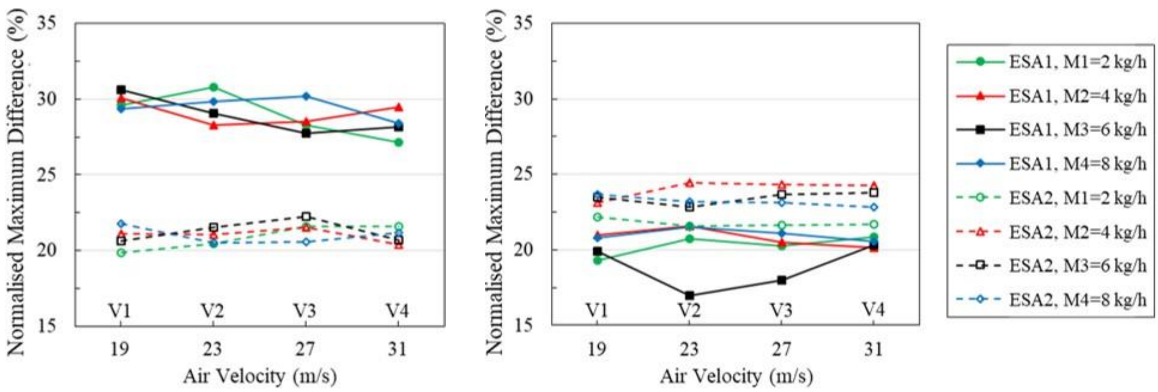

(a) (b)

Fig. 16. Normalised maximum differences of velocities measured by electrostatic sensor array 1 and electrostatic sensor array 2 under different test conditions: (a) horizontal pipe; (b) vertical pipe.

4. Conclusions

Intrusive and non-intrusive electrostatic sensor arrays in combination with the biharmonic spline interpolation method have been used to measure the cross-sectional velocity and concentration profiles of pneumatically conveyed particles in a square-shaped pipe under various dilute flow conditions. Experimental results have demonstrated that in a horizontal pipe more particles are transported in the central area at the bottom of the pipe with lower velocity than those in the two corners. While more particles are conveyed near the pipe walls than those in the centre of the pipe in a vertical pipe. Particles in the centre of both horizontal and vertical pipe cross sections travel faster compared with those close to the pipe walls. In a vertical pipe, the velocities of the particles close to the medial wall of the bend are higher than those close to the lateral wall of the bend. The mean cross-sectional particle parameters measured by the proposed electrostatic sensor array and the non-intrusive electrostatic sensor array are slightly different due to their different localised particle parameter calculation methods and the spatial sensitivity distribution. The normalised maximum difference of the RMS charge levels reduces by 4.5% for every 2 kg/h increase in particle mass flow rate and reduces by 4.6% for every 4 m/s increase in air velocity. This outcome can be extended such that the particle concentration distribution is more uniform across the pipe under higher particle mass flow rate or conveying air velocity conditions. However, the particle velocity distribution remains unchanged with particle mass flow rate or conveying air velocity. The measured particle velocity profiles show that the proposed intrusive sensor array is advantageous to the non-intrusive sensor array when measuring the local parameters of particles. Therefore, the intrusive sensor array can be used for the calibration of other electrostatic sensing systems used for flow parameter measurement in a square-shaped pipe.

Acknowledgement

This work is supported by the National Natural Science Foundation of China (No. 61603135), the Fundamental Research Funds for the Central Universities (2019MS023) granted by the North China Electric Power University and the International Clean Energy Talent Program (iCET) of the China Scholarship Council.

References

[1] Y. Zheng, Q. Liu, Review of techniques for the mass flow rate measurement of pneumatically conveyed solids, Meas. 44(2011) 589–604.

[2] S. Liu, Q. Chen, H. Wang, F. Jiang, I. Ismail, W. Yang, Electrical capacitance tomography for gas–solids flow measurement for circulating fluidized beds, Flow Meas. Instrum. 16(2005) 135–144.

[3] B. Jurjevčič, A. Senegačnik, B. Drobnič, I. Kuštrin, The characterization of pulverized-coal pneumatic transport using an array of intrusive electrostatic sensors, IEEE Trans. Instrum. Meas. 64(2015) 3434–3443.

[4] S. Kuang, M. Zhou, A. Yu, CFD-DEM modelling and simulation of pneumatic conveying: A review, Powder Technol. 365(2020) 186–207.

[5] S. Zhang, S. Wu, X. Qian, Y. Yan, Profiling of pulverized fuel flow in a square-shaped pneumatic conveying pipe using electrostatic sensor arrays, The XXII World Congress of the International Measurement Confederation (IMEKO), Belfast, UK, 3–6 Sep. 2018.

[6] S. Zhang, Y. Yan, X. Qian, Y. Hu, Mathematical modeling and experimental evaluation of electrostatic sensor arrays for the flow measurement of fine particles in a square-shaped pipe, IEEE Sens. J. 16(2016) 8531–8541.

[7] L. Peng, Y. Zhang, Y. Yan, Characterization of electrostatic sensors for flow measurement of particulate solids in square-shaped pneumatic conveying pipelines, Sens. Actuators A: Phys. 141(2008) 59–67.

[8] S. Fokeer, S. Kingman, I. Lowndes, A. Reynolds, Characterisation of the cross sectional particle concentration distribution in horizontal dilute flow conveying—a review, Chem. Eng. Process. 43(2004) 677–691.

[9] D. McGlinchey, Characterisation of Bulk Solids, CRC Press LLC, Boca Raton, USA, 2009.

[10] K. Miyazaki, G. Chen, F. Yamamoto, J.I. Ohta, Y. Murai, K. Horii, PIV measurement of particle motion in spiral gas–solid two-phase flow, Exp. Therm. Fluid Sci. 19(1999) 194–203.

[11] S. Wang, C. Xu, J. Li, Z. Ding, S. Wang, An instrumentation system for multi-parameter measurement of gas-solid two-phase flow based on Capacitance-Electrostatic sensor, Meas. 94(2016), 812–827.

[12] J. Nohlert, T. Rylander, T. McKelvey, Cavity resonator sensor and temporal signals analysis for object detection in granular flows, Meas. 150(2020), 107027.

[13] Y. Yan, Mass flow measurement of bulk solids in pneumatic pipelines, Meas. Sci. and Technol. 7(1996) 1687–1706.

[14] M.A. Mergheni, J.C. Sautet, G. Godard, H.B. Ticha, S.B. Nasrallah, Experimental investigation of turbulence modulation in particle-laden coaxial jets by Phase Doppler Anemometry, Exp. Therm. Fluid Sci. 33(2009) 517–526.

[15] A.E. Setekleiv, H.F. Svendsen, Comparison of piezo electric particle monitor with laser diffraction technique. Meas. 55(2014), 133–141.

[16] A.J. Weinheimer, The charge induced on a conducting cylinder by a point charge and its application to the measurement of charge on precipitation. J. Atmos. Ocean Technol. 5(1988) 298–304.

[17] X. Qian, D. Shi, Y. Yan, Effects of moisture content on electrostatic sensing based mass flow measurement of pneumatically conveyed particles, Powder Technol. 311(2017) 579–588.

[18] J.R. Coombes, Y. Yan, Measurement of velocity and concentration profiles of pneumatically conveyed particles using an electrostatic sensor array, IEEE Tran. Instrum. Meas. 65(2016) 1139–1148.

[19] J.B. Gajewski, Electrostatic nonintrusive method for measuring the electric charge, mass flow rate, and velocity of particulates in the two-phase gas–solid pipe flows—its only or as many as 50 years of historical evolution, IEEE Trans. Ind. Appl. 44 (2008) 1418–1430.

[20] J.F.W. Adams, M. Fairweather, J. Yao, Modelling and simulation of particle re-suspension in a turbulent square duct flow, Comp. Chem. Eng. 35(2011) 893–900.

[21] S.N. Murnane, R.N. Barnes, S.R. Woodhead, J.E. Amadi-Echendu, Electrostatic modelling and measurement of airborne particle concentration, IEEE Trans. Instrum. Meas. 45(1996) 488–492.

[22] X. Qian, Y. Yan, J. Shao, L. Wang, H. Zhou, C. Wang, Quantitative characterization of pulverised coal and biomass-coal blends in pneumatic conveying pipelines using electrostatic sensor arrays and data fusion techniques, Meas. Sci. Technol. 23(2012), 085307.

[23] S. Matsusaka, H. Maruyama, T. Matsuyama, M. Ghadiri, Triboelectric charging of powders: A review, Chem. Eng. Sci. 65 (2010) 5781–5807.

[24] T. Ken-ichiro, T. Hiroshi, K. Hajime, M. Hiroaki, Numerical simulation of tribo-electrification of particles in a gas–solids two-phase flow, Powder Technol. 118 (2001) 121–129.

[25] Y. Yan, Guide to the flow measurement of particulate solids in pipelines part 1: fundamentals and principles, Powder Handl. Process. 13(2001) 343–352.

[26] D.T. Sandwell, Biharmonic spline interpolation of GEOS-3 and SEASAT altimeter data, Geophys. Res. Lett. 14(1987) 139–142.

[27] I.L. Feliciano-Cruz, E.I. Ortiz−Rivera, Biharmonic spline interpolation for solar radiation mapping using Puerto Rico as a case of study, Proceedings of The 38th IEEE Photovoltaic Specialists Conference, Austin, TX, USA, 2012.

[28] C. Gáspár, Multigrid technique for biharmonic interpolation with application to dual and multiple reciprocity method[J]. Numer. Algorithms 21(1999) 165–183.